Thermochimica Acta 479 (2008) 53–58

Contents lists available at ScienceDirect

Thermochimica Acta

journal homepage: www.elsevier.com/locate/tca

Thermal stability of the Fe^{III}EDTA complex in its monomeric form

P.Á. Szilágyi[a,b], J. Madarász[c], E. Kuzmann[d], A. Vértes[d], G. Molnár[b],
A. Bousseksou[b], V.K. Sharma[e], Z. Homonnay[a,*]

[a] *Laboratory of Nuclear Chemistry, Eötvös Loránd University, Budapest, Hungary*
[b] *Laboratory of Coordination Chemistry of the CNRS UPR8241, Toulouse, France*
[c] *Department of Inorganic and Analytical Chemistry, Budapest University of Technology and Economics, H-1521 Budapest, Hungary*
[d] *Laboratory of Nuclear Chemistry, Chemical Research Centre of the Hungarian Academy of Sciences, Budapest, Hungary*
[e] *Laboratory of Green Chemistry, Florida Institute of Technology, Melbourne, FL, USA*

ARTICLE INFO

Article history:
Received 8 July 2008
Received in revised form 7 September 2008
Accepted 9 September 2008
Available online 24 September 2008

Keywords:
Fe-EDTA complex
Thermal degradation
Mössbauer spectroscopy
TGA
MS-coupled evolved gas analysis
Mechanism of decomposition

ABSTRACT

Thermal degradation of the solid monomeric Na[FeEDTA(H_2O)]·$2H_2O$ (EDTA = ethylenediaminetetraacetate anion) complex was studied in air by simultaneous thermogravimetry and differential thermal analysis (TG/DTA) coupled on-line with a quadrupole mass spectrometer for evolved gas analysis (EGA-MS). The solid products were analysed by Mössbauer spectroscopy. A four-step decomposition was observed until 500 °C by TG/DTA–EGA-MS, involving first the release of two molecules of crystal lattice water then one coordinated water molecule and above 200 °C, the release of CO_2 as a result of degradation of a carboxylate arm of the EDTA ligand. While releasing CO_2, reduction of the ferric iron to ferrous iron was observed by Mössbauer spectroscopy. Two ferrous species have been found to form simultaneously which are assumed to be configurational isomers since their aerial oxidation resulted in the formation of the same μ-oxo dimeric iron(III) species. Reaction pathway for this oxidation is proposed. Finally, the organic residues are burnt out rapidly accompanied by a very sharp exothermic heat effect between 280 and 330 °C; meanwhile magnetite is formed.

1. Introduction

Several studies have been carried out regarding the thermal behaviour of the hydrated sodium ethylenediaminetetraacetato ferrate(III) complex, $NaFe^{III}EDTA_{aq}$, especially because of the possible applications in dissolving iron oxides by the help of ethylenediaminetetraacetic acid containing solutions [1–6]. These methods are more efficient at higher temperatures but the possible degradation of the chelating agent or the complex should be taken into account. Studies found in the literature mostly dealt with the investigation of the thermal behaviour under hydrous conditions [7–9], but attempts to describe the thermal behaviour of the complex in solid state using TG and DTA measurements have also been done [10,11].

The crystal structure of our solid title compound, sodium aqua[ethylenediaminetetra-acetato-N,N′,O,O′,O″,O‴]iron(III) dihydrate (Na[Fe($C_{10}H_{12}N_2O_8$)(H_2O)]·$2H_2O$) was determined first by Novozhilova et al. [12] in space group *B11b* (R = 11.8%) and independently at the same time by Solans et al. [13] (R = 4.7%) and López-Alcalá et al. [14] (R = 2.7%) in space group *Cc*, as a hepta-coordinated complex with one water molecule in the inner coordination sphere of iron [15].

Thermogravimetry (TG) is a useful method to distinguish water molecules bound in solid hydrated complexes with various strengths [16]. First Hall and Lambert [17] reported, that the thermogravimetric analysis of Na[Fe(H_2O)EDTA]·$2H_2O$ in flowing N_2 up to 325 °C showed three-step decomposition, which they assigned to the loss of directly coordinated and non-coordinated water as well as carbon dioxide, however no TG-curve was published. Two-step TG-curve of the title compound up to 200 °C was presented by Martynenko et al. [18]. More recently, El-Dien [19] reported separate TG and differential thermal analysis (DTA) of a sodium Fe-EDTA monohydrate prepared from iron(III) sulphate, but the formula, figures and discussion seem to be contradictory and rather spurious. For example, only evolution of carbon dioxide was suggested and not that of water, without any type of evolved gas analysis.

In this paper, results of a simultaneous TG/DTA investigation coupled online with mass spectrometric evolved gas analysis (EGA-MS) on Na[Fe(H_2O)EDTA]·$2H_2O$ is reported. Combining these methods with Mössbauer spectroscopy makes the study of the thermal degradation of this compound possible with parallel tracking of the fate of iron in the solid state. Since Mössbauer spectroscopy has an extreme sensitivity for slight changes in the coordination sphere of iron ions (*e.g.* increase or decrease in the coordination

---

* Corresponding author. Tel.: +36 1 3722569; fax: +36 1 3722567.
E-mail address: homonnay@ludens.elte.hu (Z. Homonnay).

doi:10.1016/j.tca.2008.09.009

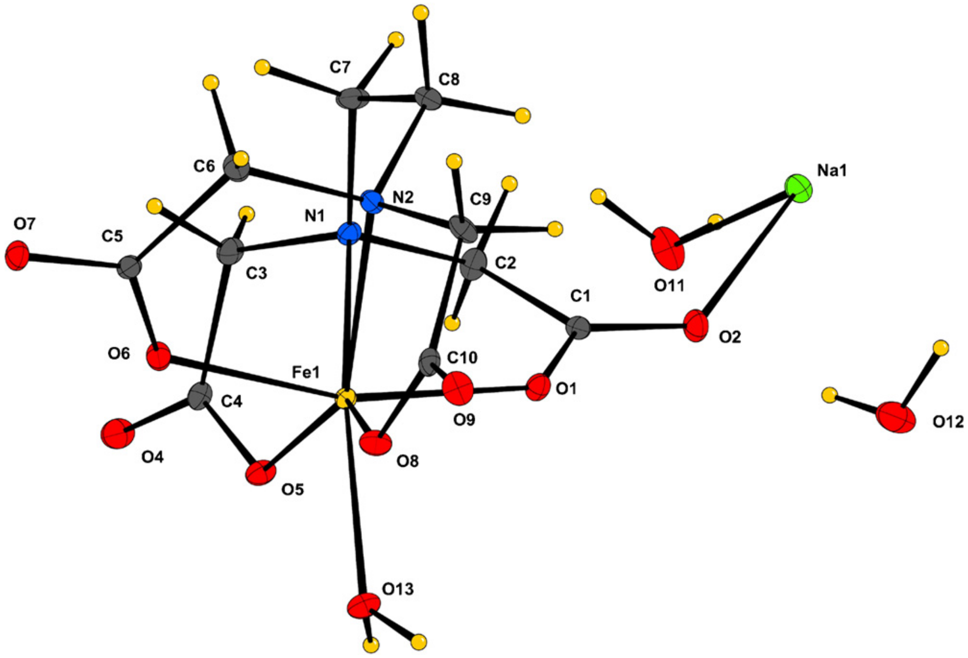

Fig. 1. Structure of NaFeEDTA(H_2O)·$2H_2O$ indicating also the crystal water molecules as determined from a single crystal X-ray diffractogram recorded at 180 K.

number, distortion of the coordination polyhedron, exchange of ligands), effects of thermal treatments on the iron-complex can be studied efficiently, possible transitional states of iron may be detected, which can reveal so far unknown details of the degradation mechanism. Although Mössbauer studies have been reported on this system after thermal treatments [20] a systematic and thermal analysis coupled investigation has not been done yet.

2. Experimental

Na[FeEDTA(H_2O)]·$2H_2O$ was purchased from Sigma–Aldrich (98%). Its XRD (X'pert Pro MPD X-ray diffractometer, Cu Kα radiation, Ni-filter) profile has confirmed the crystalline phase present, through identification with PDF file No. 00-36-1828 [21], and also with generated powder patterns corresponding to the single crystal structure determination of Refs. [13–15,22], as sodium aqua ethylenediaminetetraacetato(4-) ferrate dihydrate. The CHN-elemental analysis (Heraus Rapid CHN-O Analyser) showed the following percentage of carbon, nitrogen, and hydrogen: C% 28.72, N% 6.61, and H% 4.19 (calculated for the formula $NaC_{10}H_{18}FeN_2O_{11}$: C% 28.52, N% 6.65, and H% 4.31).

For single crystal XRD measurements, data collection and cell refinement were carried out with a sealed Mo Kα ($\lambda = 0.71073$ Å) X-ray source on an Oxford Xcalibur diffractometer using the Crysalis softwares [23] at 180 K. The structure was solved using SIR92 [24], whereas the refinement was done by the help of the SHELXL-97 [25] softwares. Calculations were performed using the WINGX programme package [26]. Molecular structure was drawn with ORTEP [27]. Atomic scattering factors were taken from the International Tables for X-ray Crystallography [28].

The selection of the temperature for thermal treatments was based on simultaneous TG/DTA measurements of the salt carried out in an STD 2960 Simultaneous DTA–TGA apparatus (TA Instruments Inc., USA), at a heating rate of 10 K/min, an air flow rate of 130 ml/min. Initial sample masses were between 10 and 12 mg, and an open Al crucible was used.

For evolved gas analysis, the mixture of gaseous species yielded from the above simultaneous TG/DTA instrument could reach a ThermoStar GDS 200 (Balzers Instruments) quadrupole mass spectrometer equipped with Chaneltron detector, through a heated 100% methyl deactivated fused silica capillary tubing kept at $T = 200\,^{\circ}C$. Data collection was carried out with QuadStar 422v60 software in multiple ion detection mode (MID) monitoring 64 selected channels ranging mostly between $m/z = 12–78$. Measuring time was *ca.* 0.5 s for one channel, resulting in time of measuring cycles of *ca.* 30 s.

The Mössbauer measurements were carried out with a conventional Mössbauer spectrometer in constant acceleration mode. $^{57}Co(Rh)$ sources were used, the isomer shifts are converted so that they refer to α-iron at room temperature. Spectrum evaluations have been done using the MossWinn3.0 software package [29].

3. Results and discussion

Single crystal structure of the Na[FeEDTA(H_2O)]·$2H_2O$ was recorded at 180 K (see Fig. 1), parameters are listed in Table 1. Fig. 2 displays the crystal structure packing of the same compound. Bond lengths and angles are listed in Supplementary Materials. The data correspond well that reported earlier [13,14] taking into account the temperature difference (180 K *vs.* room temperature).

The thermal behaviour of the dark yellow coloured Na[FeEDTA(H_2O)]·$2H_2O$ complex was studied in two steps; firstly, simultaneous TG/TDA–EGA-MS measurements were carried out to determine the decomposition steps, the corresponding mass losses, and evolved gases and secondly, the decomposition products were analysed using Mössbauer spectroscopy. The decomposition curves and the characteristic ion current are displayed in Figs. 3 and 4, respectively.

The relative mass losses indicate that, at 129 °C two water molecules are removed from the crystal lattice, which is followed by the release of the third water molecule at 196 °C. This difference in temperatures is reasonable, since the first two H_2O molecules are only weakly bound in the lattice, while the third molecule is coordinated to the ligand sphere of iron. The third step, at 259 °C, can be assigned to the loss of a CO_2 molecule, the source of which is a carboxylate arm of the EDTA chelating agent. This latter step

Table 1
Crystal data and structural refinement for NaFeEDTA(H_2O)·2H_2O.

Empirical formula	$NaC_{10}H_{18}FeN_2O_{11}$	Volume	1554.1(5) $Å^3$
Formula weight	421.10 g/mol	Z	4
Temperature	180 K	Calculated density	1.800 Mg/m^3
λ	0.71073 Å	μ	1. 063 mm^{-1}
Crystal system, space group	Monoclinic, *C1c1*	Crystal size	0.35 mm × 0.15 mm × 0.1 mm
Unit cell dimensions	a = 8.8881(18) Å, α = 90°, b = 11.846(2) Å,	R, R_W	0.0219, 0.0550
	β = 99.92(3)°, c = 14.985(3) Å, γ = 90°	(Δ, ρ) max, min	0.253; −0.423 e $Å^{-3}$

should be accompanied by a change in the oxidation state of the iron ions (reduction step), since the formation of a carbon dioxide molecule from a carboxylate ligand needs an electron transfer. This third degradation step is exothermic. In addition, the fourth degradation step has an even larger exothermic effect as a result of the oxidative burning of organic residues and formation of Fe_3O_4, this latter verified by XRD phase analysis.

As can be seen in Fig. 3, three degradation products are distinguishable, namely, the $NaFe^{III}EDTA \cdot H_2O$, without any crystal water molecules, the fivefold coordinated $NaFe^{III}EDTA$ complex, after the release of its coordination water molecule, and a Fe^{2+} complex resulting from the loss of CO_2 of the $NaFe^{III}EDTA$ complex.

For the Mössbauer study, thermal treatments were carried out in a temperature-controlled furnace. The temperature and duration of the treatments were 130 °C for 20 min, 200 °C for 20 min and 220 °C for 40 min, following the thermal analysis curve. The mass losses were verified before and after each treatment using a balance and a part of the resulting powder was placed into molten paraffin to avoid contact with moisture and oxygen, while the rest was kept as a powder sample to study further reactions of the degradation products. The colour of the heated powder changed after the heat treatment at 220 °C to brown.

Mössbauer spectra recorded before and after the heat treatment at 130 °C for 20 min are shown in Fig. 5(a) and (b). All spectrum parameters and errors are listed in Table 2.

The asymmetric character of the Mössbauer spectrum of solid NaFeEDTA(H_2O)·2H_2O was first reported by Spijkerman et al. [30] and was explained by a magnetic relaxation effect [31].

As can be seen in Fig. 5(a) and (b), the loss of the two crystal water molecules does not affect considerably the resultant spectrum (Fig. 5(b)); the hyperfine parameters remained similar after the heating. This means that the presence or absence of the water molecules in the crystal lattice does not affect the hyperfine interactions of the ^{57}Fe nucleus.

Mössbauer spectrum recorded after the heat treatment at 200 °C for 20 min is shown in Fig. 5(c). The lower isomer shift of the subspectrum which we can assign to the $NaFe^{III}EDTA$ species in Fig. 5(c) corresponds well to the fact that one water molecule has

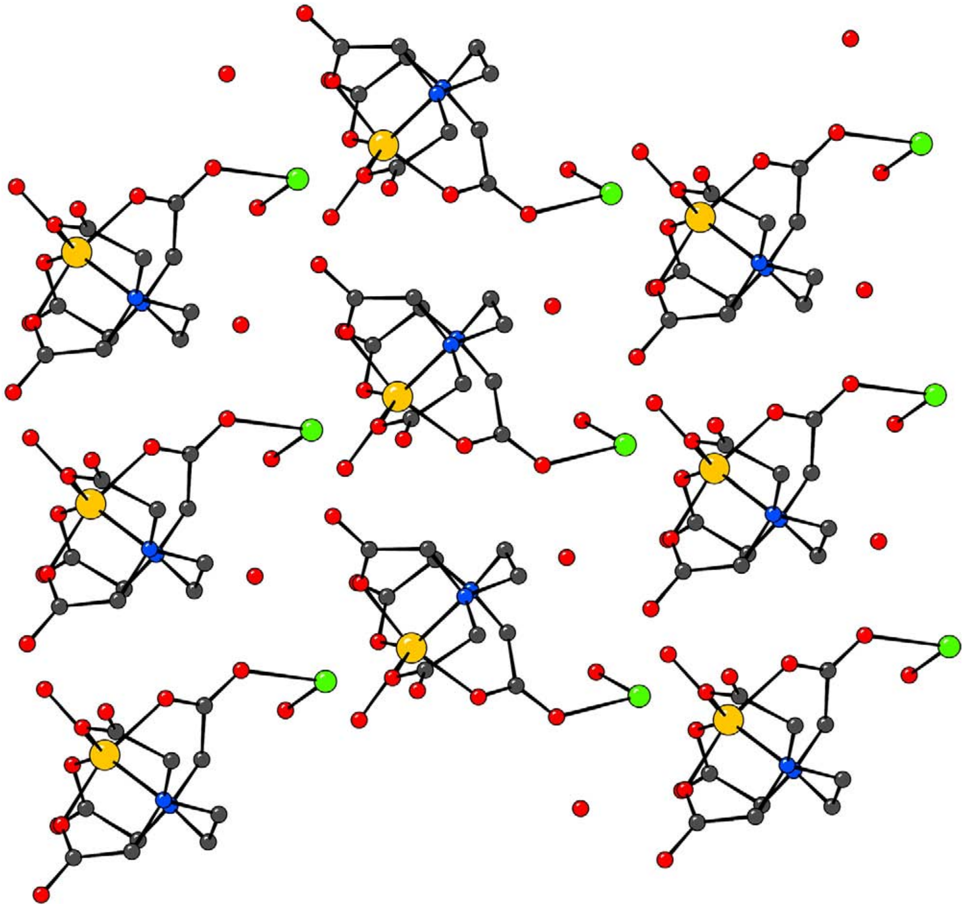

Fig. 2. Crystal structure packing for the NaFeEDTA(H_2O)·2H_2O complex at 180 K.

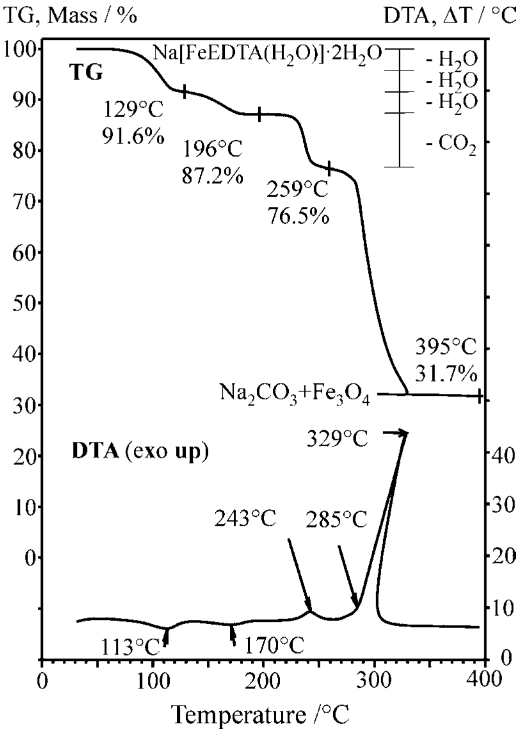

Fig. 3. Simultaneous TG/DTA curves of the Na[FeEDTA(H_2O)]·$2H_2O$ solid complex in TG/DTA-MS measurement.

been ejected from the ligand sphere of iron. This decrease in the isomer shift can be explained by the decrease of the 3d electron density (compared to the case of the NaFeEDTA(H_2O) complex, see in Fig. 5(b)), which is an indication of the decrease in the coordination number (from 7 to 6). Furthermore, the relaxation is also stopped, which is indicated by the disappearance of the doublet asymmetry.

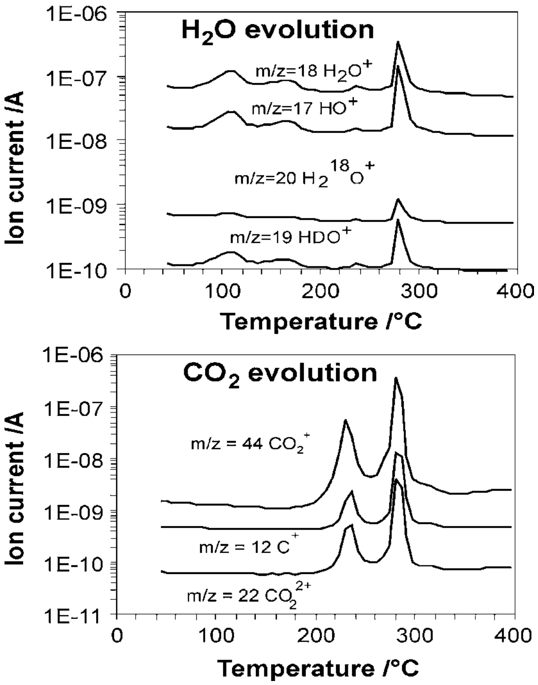

Fig. 4. Characteristic ion current *vs.* *T* at different detection channels corresponding to the evolution of water and CO_2 from the Na[FeEDTA(H_2O)]·$2H_2O$ solid complex in TG/DTA-MS measurement.

The spectrum recorded after the heat treatment at 220 °C for 40 min is displayed in Fig. 5(d). A fraction of the resultant powder was placed in molten paraffin to preserve it from contact with moisture and carbon dioxide, while, to study its oxidative degradation reactions, another fraction was kept in air and Mössbauer spectra were recorded one and ten days after the heat treatment, which are shown in Fig. 5(e) and (f), respectively.

Fig. 5(d) shows two quadrupole doublets, both referring to high spin, Fe^{2+}-bearing species. However, according to the degradation

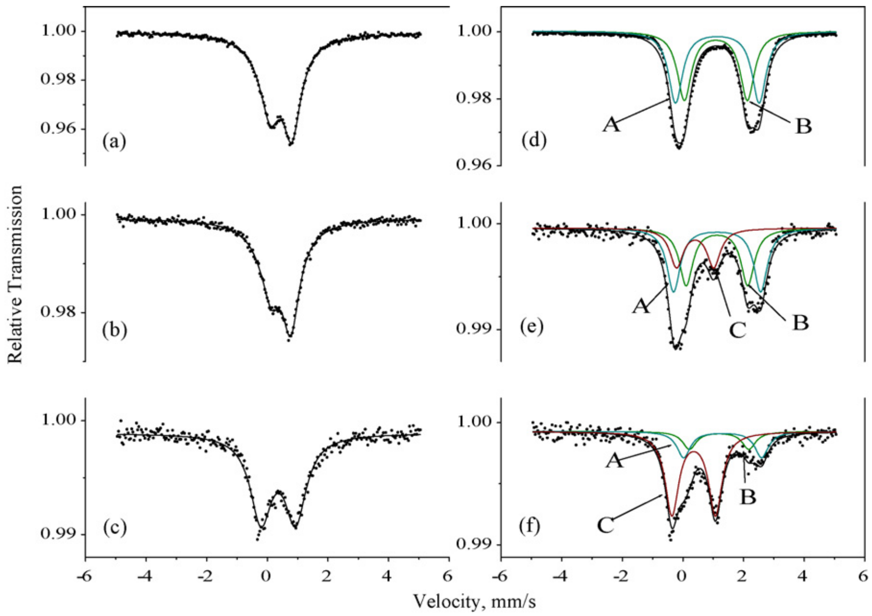

Fig. 5. Mössbauer spectra of the $NaFe^{III}EDTA·3H_2O$ complex before heat treatment (a), after the heat treatment at 130 °C for 20 min (b), after the heat treatment at 200 °C for 20 min (c), and after the heat treatment at 220 °C for 40 min (d). Sample placed into molten paraffin immediately after the heating process (d); powdered sample kept in open air for 1 day after the heat treatment (e); powdered sample kept in open air for 10 days after the heat treatment (f). All spectra were recorded at room temperature.

Table 2
Mössbauer parameters and their errors for spectra of the $NaFe^{III}EDTA{\cdot}3H_2O$ complex and of its thermal degradation products.

	Spectrum component	Proportion (%)	δ (mm/s)	eQV_{zz} (mm/s)	$\|\Delta\|$ (mm/s)	Γ (mm/s)
Fig. 5(a)[a]	–	–	0.45(1)	−0.70(1)	–	0.60(1)
Fig. 5(b)[a]	–	–	0.46(2)	−0.62(1)	–	0.50(1)
Fig. 5(c)	–	–	0.35(1)	–	1.12(1)	0.58(1)
Fig. 5(d)	A	48.9	1.08(1)	–	2.08(1)	0.56(1)[b]
	B	51.1	1.13(1)	–	2.76(1)	0.56(1)[b]
Fig. 5(e)	A	35.9	1.12(1)	–	2.03(2)	0.53(1)[b]
	B	40.0	1.12(1)	–	2.87(2)	0.53(1)[b]
	C	24.1	0.40(2)	–	1.22(8)	0.53(1)[b]
Fig. 5(f)	A	14.1	1.19(3)	–	1.96(8)	0.54(1)[b]
	B	20.7	1.2(2)	–	2.7(2)	0.54(1)[b]
	C	65.2	0.35(1)	–	1.41(1)	0.54(1)[b]

δ: isomer shift; eQV_{zz}: quadrupole shift; Δ: quadrupole splitting; Γ: full-linewidth at half-maximum.

[a] Spectrum evaluations were done using the Blume–Tjon magnetic relaxation model [32].

[b] Linewidths were constrained to be the same value within each spectrum evaluation.

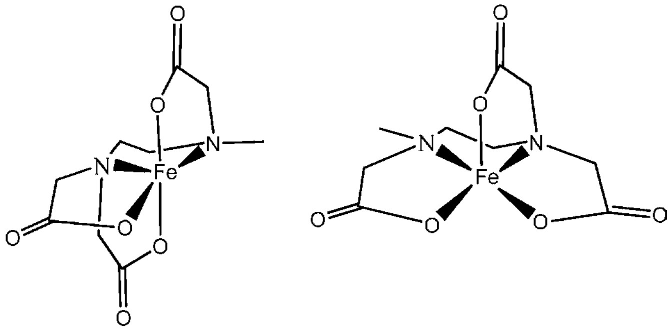

Fig. 6. Proposed structures for the two ferrous species formed in the course of thermal degradation of $NaFeEDTA(H_2O){\cdot}2H_2O$.

pathway, namely that one carboxylate arm gets detached in the course of the decomposition of the $NaFeEDTA(H_2O){\cdot}2H_2O$ complex, the formation of only one ferrous degradation product was expected. The isomer shifts of the two distinct subspectra.[1] are the same and their area ratio is nearly 1:1 Since the thermal analysis curve does not display any other mass change, and the two subspectra differ only in their quadrupole splittings, we can assume that these two species, represented by subspectra A and B, formed simultaneously and they are configurational isomers. Two possible structures (more or less distorted trigonal bipyramidal and square pyramidal) for species A and B are shown in Fig. 6. These structures are the two extremes taking into account that the complex had been in a distorted octahedral environment before the ethylenediaminetetraacetate chelating agent lost one carboxylate arm.

This scenario explains the identical isomer shifts and the different quadrupole splittings.

This hypothesis is also supported by the fact that identical products are formed in the course of the aerial oxidation of both ferrous compounds.

The iron(II) compounds resulted from the ejection of a CO_2 molecule from the EDTA chelating agent, which had to be accompanied by a reduction step converting the Fe^{III} form into Fe^{II}. The oxidation of the ferrous compounds was carried out by aerial oxygen. This reaction might take place in the following way: an oxygen molecule binds to the ligand sphere of iron(II) ($\{[Fe^{II}L]^-\}\xrightarrow{O_2}\{O_2[Fe^{II}L]^-\}$), oxidises it by internal electron transfer (ET) ($\{O_2[Fe^{II}L]^-\}\xrightarrow{ET}\{O_2[Fe^{III}L]^-\}$), then it binds another ferrous entity building a bridge ($\{O_2[Fe^{III}L]^-\}\xrightarrow{\{[Fe^{II}L]^-\}}\{[LFe^{II}(O_2)Fe^{III}L]^{2-}\}$), oxidises this second ferrous part as well ($\{[LFe^{II}(O_2)Fe^{III}L]^{2-}\}\xrightarrow{ET}\{[LFe^{III}(O_2)Fe^{III}L]^{2-}\}$), and an oxygen atom is then released from the bond ($\{[LFe^{III}(O_2)Fe^{III}L]^{2-}\}\xrightarrow{-O:}[LFe^{III}{-}O{-}Fe^{III}L]^{2-}$), leaving a μ-oxo bridged dimer behind in the crystal lattice (L denotes the N′-methyl-ED3A (N,N,N′-ethylenediaminetriacetate) ligand). Note that the proposed fivefold coordination of the ferrous entities facilitates the coordination of an O_2 molecule or an oxygen atom (radical).

This hypothesis (formation of the dimer species) is reinforced by the hyperfine parameters of the subspectrum describing the oxidised form of the degradation products being very close to those of the dimeric $Fe^{III}EDTA$ ($\delta = 0.36$ mm/s, $\Delta = 1.60$ mm/s at room temperature and $\delta = 0.44$ mm/s, $\Delta = 1.60$ mm/s at 80 K [32,33]). The relatively high quadrupole splitting value (1.41 mm/s) for these spectra can be due to the angle of the Fe–O–Fe bonds being presumably close to 180° (very tense structure).

4. Conclusions

The thermal degradation products of the monomeric $NaFeEDTA{\cdot}3H_2O$ complex as well as their oxidation products were identified. First the crystal water molecules evaporated, and then the coordinated water molecule was released. The third step of the thermal decomposition is the detachment of a coordinated carboxylate arm, followed by the formation of a CO_2 molecule. This process is known to result in a change in the oxidation state of the iron ion, *i.e.* when the carbon atom is oxidised, the ferric ion is reduced to ferrous ion. Two ferrous species have been found to form in the course of this degradation step. These two species are assumed to be configurational isomers. This hypothesis is based on the reasoning that the isomer shifts of the two doublets representing the two ferrous compounds are identical, and that the oxidation product of the two ferrous compounds is the same ferric species. The further oxidation product of the two resultant ferrous degradation products has been recognised as a μ-oxo dimeric species on the basis of the hyperfine parameters. Reaction pathway for this oxidation has also been proposed.

---

[1] It should be mentioned that the evaluation of the spectrum displayed in Fig. 5(d) may also be possible by only one ferrous doublet, however, the linewidth of the two lines of the doublet would then be different and extremely large (~0.9 mm/s). Such a distortion would only appear in relaxation phenomena but it is very unlikely for Fe^{II}. Furthermore, in the spectra present in Fig. 5(e) and (f), the ratio of the subspectra assumed to describe two ferrous entities shows no variation with time, although conditions for relaxation would certainly have to change with the heat treatments. This also supports the two doublet model for evaluation.

Acknowledgements

This work has been sponsored by the Hungarian National Science Fund (OTKA) and National Agency for Research and Technology (NKTH), grant numbers K-67835, K-62691. V.K. Sharma and Z. Homonnay acknowledge the support U.S.-Hungary Partnership Program (NSF-MTA-OTKA 85-46138). Petra Ágota Szilágyi would like to express her acknowledgments to the Embassy of France in Hungary for her PhD scholarship. The authors thank Mrs. H. Medzihradszky for the elemental analysis.

Appendix A. Supplementary data

Supplementary data associated with this article can be found, in the online version, at doi:10.1016/j.tca.2008.09.009.

References

[1] M.I. Litter, E.C. Baumgartner, G.A. Urrutia, M.A. Blesa, Environ. Sci. Technol. 25 (1991) 1907–1913.
[2] M.I. Litter, M.A. Blesa, J. Colloid Interface Sci. 125 (1988) 679–687.
[3] R. Torres, M.A. Blesa, E. Matijević, J. Colloid Interface Sci. 131 (1989) 567.
[4] G. Karametaxas, S.J. Hug, B. Sulzberger, Environ. Sci. Technol. 29 (1995) 2992–3000.
[5] E. Baumgartner, M.A. Blesa, H.A. Marinovich, A.J.G. Maroto, Inorg. Chem. 22 (1983) 2224–2226.
[6] M.A. Blesa, H.A. Marinovich, E.C. Baumgartner, A.J.G. Maroto, Inorg. Chem. 26 (1987) 3713–3717.
[7] N.I. Kuz'menko, E.M. Yakimets, Zh. Khim. 190 (1973) 76–83.
[8] E.M. Yakimets, N.A. Berg, N.I. Kuz'menko, Teploenergetika 18 (1971) 84–85.
[9] Chemical cleaning of thermal power equipment, in: T.H. Margulova (Ed.), Energia, 1969, Moscow.
[10] J. Garcia-Oricain, A. Fuster, Afinidad XXXIX (1982) 541–542.
[11] F.A. Nour El-Dien, Spectrosc. Lett. 32 (1999) 407–419.
[12] N.V. Novozhilova, T.N. Polynova, M.A. Porai-Koshits, Zh. Strukt. Khim. (Russ.) (J. Struct. Chem.) 16 (1975) 865–874.
[13] X. Solans, M. Font Altaba, J. Garcia-Oricain, Acta Crystallogr., Sect. C: Cryst. Struct. Commun. C40 (1984) 635–638.
[14] J.M. López-Alcalá, M.C. Puerta-Vizcaíno, F. González-Vílchez, Duesler, N. Eileen, R.E. Tapscott, Acta Crystallogr., Sect. C: Cryst. Struct. Commun. C40 (1984) 939–941.
[15] F.H. Allen, Acta Crystallogr. B58 (2002) 380–388.
[16] F. Paulik, Special Trends in Thermal Analysis, Wiley, New York, 1995.
[17] L.H. Hall, J.L. Lambert, J. Am. Chem. Soc. 90 (1968) 2036–2039.
[18] L.I. Martynenko, N.I. Pechurova, V.I. Spitsyn, A. Hadi, K.I. Popov, Nguyen-Dinh-Ngo, Izv. Akad. Nauk SSSR, Ser. Khim. (Russ.) 12 (1970) 2659–2664.
[19] F.A.N. El-Dien, Spectrosc. Lett. 32 (1999) 407–419.
[20] M. Takeda, Hyperfine Interact. 28 (1986) 737–740.
[21] International Centre for Diffraction Data (ICDD), Powder Diffraction File PDF-2 Release, 2007.
[22] C.F. Macrae, P.R. Edgington, P. McCabe, E. Pidcock, G.P. Shields, R. Taylor, M. Towler, J. van de Streek, J. Appl. Crystallogr. 39 (2006) 453–457.
[23] CrysAlis CCD, version 1.171.24, Xcalibur CCD system, Oxford Diffraction, 2004.
[24] A. Altamore, G. Cascarano, G. Giacovazzo, A. Guargliardi, M.C. Burla, G. Polidori, M. Camalli, J. Appl. Cryst. 27 (1994) 435–1435.
[25] G.M. Sheldrick, SHELXL-97—Programs for Crystal Structure Analysis (Release 97-2), Göttingen, Germany, 1997.
[26] L.J. Farrugia, J. Appl. Cryst. 32 (1999) 837–838.
[27] T. Hahn (Ed.), International Tables for Crystallography, Kluwer Academic Publishers, Dordrecht, The Netherlands, 1995.
[28] L.J. Farrugia, J. Appl. Cryst. 30 (1997) 565–566.
[29] Z. Klencsár, E. Kuzmann, A. Vértes, J. Radioanal. Nucl. Chem. 210 (1996) 105–118.
[30] J.J. Spijkerman, L.H. Hall, J.L. Lambert, J. Am. Chem. Soc. 90 (1968) 2039–2043.
[31] M. Blume, J.A. Tjon, Phys. Rev. 165 (1968) 446–461.
[32] A. Márton, N. Sükösd-Rozlosnik, A. Vértes, I. Nagy-Czakó, K. Burger, Inorg. Chim. Acta 137 (1987) 173–176.
[33] H.J. Schugar, G.R. Rossman, C.D. Barraclough, H.B. Gray, J. Am. Chem. Soc. 21 (1972) 2683–2690.